Tristetraprolin regulation of interleukin 23 mRNA stability prevents a spontaneous inflammatory disease

Céline Molle,[1] Tong Zhang,[1] Laure Ysebrant de Lendonck,[1] Cyril Gueydan,[2] Mathieu Andrianne,[1] Félicie Sherer,[3,4] Gaetan Van Simaeys,[3,4] Perry J. Blackshear,[5,6] Oberdan Leo,[1] and Stanislas Goriely[1,7]

[1]Institute for Medical Immunology (IMI), [2]Laboratoire de Biologie Moléculaire du Gène, and [3]Center for Microscopy and Molecular Imaging (CMMI), Université Libre de Bruxelles, B-6041 Charleroi-Gosselies, Belgium
[4]Department of Nuclear Medicine, Hôpital Erasme, Université Libre de Bruxelles, B-1070 Brussels, Belgium
[5]The Laboratory of Signal Transduction, National Institute of Environmental Health, National Institutes of Health Sciences, Research Triangle Park, NC 27709
[6]Departments of Medicine and Biochemistry, Duke University Medical Center, Durham, NC 27710
[7]WELBIO, B-6041 Charleroi-Gosselies, Belgium

Interleukin (IL) 12 and IL23 are two related heterodimeric cytokines produced by antigen-presenting cells. The balance between these two cytokines plays a crucial role in the control of Th1/Th17 responses and autoimmune inflammation. Most studies focused on their transcriptional regulation. Herein, we explored the role of the adenine and uridine–rich element (ARE)–binding protein tristetraprolin (TTP) in influencing mRNA stability of IL12p35, IL12/23p40, and IL23p19 subunits. LPS-stimulated bone marrow–derived dendritic cells (BMDCs) from TTP$^{-/-}$ mice produced normal levels of IL12/23p40. Production of IL12p70 was modestly increased in these conditions. In contrast, we observed a strong impact of TTP on IL23 production and IL23p19 mRNA stability through several AREs in the 3′ untranslated region. TTP$^{-/-}$ mice spontaneously develop an inflammatory syndrome characterized by cachexia, myeloid hyperplasia, dermatitis, and erosive arthritis. We observed IL23p19 expression within skin lesions associated with exacerbated IL17A and IL22 production by infiltrating γδ T cells and draining lymph node CD4 T cells. We demonstrate that the clinical and immunological parameters associated with TTP deficiency were completely dependent on the IL23–IL17A axis. We conclude that tight control of IL23 mRNA stability by TTP is critical to avoid severe inflammation.

CORRESPONDENCE
Stanislas Goriely:
stgoriel@ulb.ac.be

Abbreviations used: ARE, adenine and uridine–rich element; BMDC, BM-derived DC; dLN, draining LN; EAE, experimental autoimmune encephalomyelitis; HEK, human embryonic kidney; TTP, tristetraprolin; UTR, untranslated region.

IL12 and IL23 play crucial and distinct roles in shaping the innate and adaptive immune responses against invading pathogens. Furthermore, imbalanced expression of these two cytokines can lead to autoimmune or inflammatory disorders. Indeed, experimental models highlighted the pathogenic role of IL23 in the development of arthritis, experimental autoimmune encephalomyelitis (EAE), psoriasis, or inflammatory bowel disease (Kastelein et al., 2007). Although a protective role of IL12 has been demonstrated in the course of EAE and arthritis, this cytokine plays a detrimental role in some autoimmune diseases such as colitis (Kastelein et al., 2007). Therefore, a tightly regulated production of these two cytokines is essential to maintain homeostasis.

IL12 and IL23 are heterodimeric cytokines, composed of a common IL12/23p40 subunit and a specific α-subunit (IL12p35 and IL23p19, respectively). Produced in large excess over p35 and p19 subunits, the p40 subunit also forms homodimers. The transcriptional activation of IL12 family has been extensively studied. TLR ligands are major inducers of the synthesis of IL12 family members. The balance between bioactive IL12p70 and IL23 is affected by the type of TLR that is engaged and additional signals such as type I and type II IFNs, mainly

The Rockefeller University Press $30.00
J. Exp. Med. 2013 Vol. 210 No. 9 1675-1684
www.jem.org/cgi/doi/10.1084/jem.20120707

The Journal of Experimental Medicine

through differential involvement of interferon regulatory factors (Goriely et al., 2008). Engagement of other pattern recognition receptors also influences this balance. For example, signaling through C-type lectins and NOD (nucleotide-binding oligodimerization domain) strongly favors IL23 production (Gerosa et al., 2008). In addition to transcriptional regulatory networks, dynamic expression of cytokine and chemokine genes is strongly influenced by mRNA decay (Hao and Baltimore, 2009). Indeed, 3′ untranslated regions (UTRs) of these genes are enriched in adenine and uridine–rich elements (AREs), sequences which control mRNA stability and translation through recruitment of protein complexes (Blackshear, 2002). Tristetraprolin (TTP; encoded by *Zfp36*) is one of the best-characterized ARE-binding protein. TTP limits the production of several TLR-induced cytokines, including TNF, IL6, GM-CSF, and CCL3 (Lai et al., 1999; Carballo et al., 2000; Kang et al., 2011; Van Tubergen et al., 2011). Recently, transcriptome analyses indicate that out of 546 LPS-inducible transcripts in macrophages, 138 were found to be unstable. Expression of one third (45) of these mRNAs was affected by the absence of TTP (Kratochvill et al., 2011).

TTP deficiency leads to the spontaneous development of a complex inflammatory syndrome, characterized by severe cachexia, dermatitis, arthritis, and myeloid hyperplasia (Taylor et al., 1996). Although TNF plays a critical pathogenic role in these settings, the phenotype of these mice remains incompletely understood, probably as a result of the large number of potential TTP targets. In this study, we investigated the contribution of TTP in the control of IL12 and IL23 balance. We show that IL23p19 is a preferential target of TTP and plays a major role in the development of the TTP deficiency syndrome.

RESULTS AND DISCUSSION

Absence of TTP results in IL23 overproduction by LPS-stimulated BMDCs

We identified several AREs within the 3′UTR regions of human and murine IL12p35, IL12/23p40, and IL23p19 mRNAs, suggesting that these genes could be regulated at the posttranscriptional level. In a first set of experiments, we generated BM-derived DCs (BMDCs) from WT or $TTP^{-/-}$ mice to assess the impact of this ARE-binding protein on IL12 and IL23 production in response to TLR ligands such as LPS (TLR4 ligand). In comparison with their WT counterparts, $TTP^{-/-}$ BMDC cells produced fourfold higher levels of IL23. Although IL12p70 levels were also increased in $TTP^{-/-}$ BMDCs, the observed differences did not reach statistical significance (Fig. 1 A). In marked contrast, production of IL12/23p40 was comparable in both groups. We reached similar conclusions when BMDCs or macrophages were stimulated with TLR7/8 ligand (R848), TLR9 ligand (CpG), or an LPS+R848 combination (unpublished data). Next, we analyzed the impact of TTP on steady-state mRNA levels. In WT BMDCs, IL23p19 mRNA was rapidly and transiently expressed, reaching peak concentrations 2 h after stimulation before returning to near-baseline levels 6 h later. IL23p19 mRNA levels were strongly increased and maintained for a longer timeframe in $TTP^{-/-}$ cells. We also observed higher IL12p35 mRNA levels in $TTP^{-/-}$ versus WT BMDCs, but kinetics were similar in both groups. Finally, consistent with protein production, absence of TTP did not affect IL12/23p40 mRNA levels (Fig. 1 B).

To analyze the impact of APC-expressed TTP on IFN-γ and IL17 production, splenocytes from TLR4 KO mice were incubated in the presence of supernatants from control or LPS-activated $TTP^{+/+}$ or $TTP^{-/-}$ BMDCs. Supernatants from LPS-stimulated $TTP^{-/-}$ BMDCs were found to promote increased IL17A and IFN-γ productions when compared with supernatants from their WT counterparts (Fig. 1 C). Addition of both anti-p40 and anti-p19 neutralizing antibodies blocked IL17 production, whereas only antibodies directed against p40 were able to inhibit IFN-γ production (Fig. 1 D), confirming the molecular identity and bioactivity of, respectively, IL23 and IL12 . Collectively, these results indicate that TTP is implicated in the negative regulation of IL23p19 and, to a lesser extent, of IL12p35 mRNA expression. In the absence of TTP, overproduction of bioactive IL23 and IL12 has a functional impact on the production of IL17 and IFN-γ, respectively.

TTP regulates IL23p19 mRNA stability via multiple AREs within the 3′UTR

To assess the role of TTP in the control of IL12p35 and IL23p19 mRNA stability, we analyzed the mRNA half-lives of these subunits. Blockade of transcription by actinomycin D led to a rapid decay of IL12p35 mRNAs in both $TTP^{+/+}$ and $TTP^{-/-}$ BMDCs, whereas IL12/23p40 and IL23p19 mRNA levels were found to be stable in both groups (unpublished data). To reveal an effect of TTP, we treated cells with actinomycin D and SB2202190, a p38-MAPK inhibitor used to abrogate the inhibitory action of p38-MAPK on TTP activation (Carballo et al., 2001). The presence of both inhibitors resulted in the rapid destabilization of IL23p19 mRNA, which was completely attributable to TTP. Addition of the p38-MAPK inhibitor further accelerated IL12p35 mRNA decay in a TTP-dependent manner but did not modify IL12/23p40 mRNA levels (Fig. 1 E).

The presence of AREs in the 3′UTRs is known to cause rapid decay of the corresponding mRNAs, resulting in a tightly controlled secretion of many inflammatory mediators (Anderson, 2008). Because IL23p19 mRNA contains five AREs within its 3′UTR (Fig. 1 H), we decided to evaluate the role of this region in the control of p19 mRNA degradation. Interestingly, four of these AREs were conserved in the 3′UTR region of the human IL23p19 mRNA, suggesting that they might play an important role. We cloned the p19 3′UTR immediately downstream of the mIL2 coding sequence and transfected this reporter construct into HEK-293 cells. mIL2 production was greatly reduced in cells transfected with the 3′UTRp19-containing plasmid, consistent with the notion that 3′UTRp19 displays regulatory functions

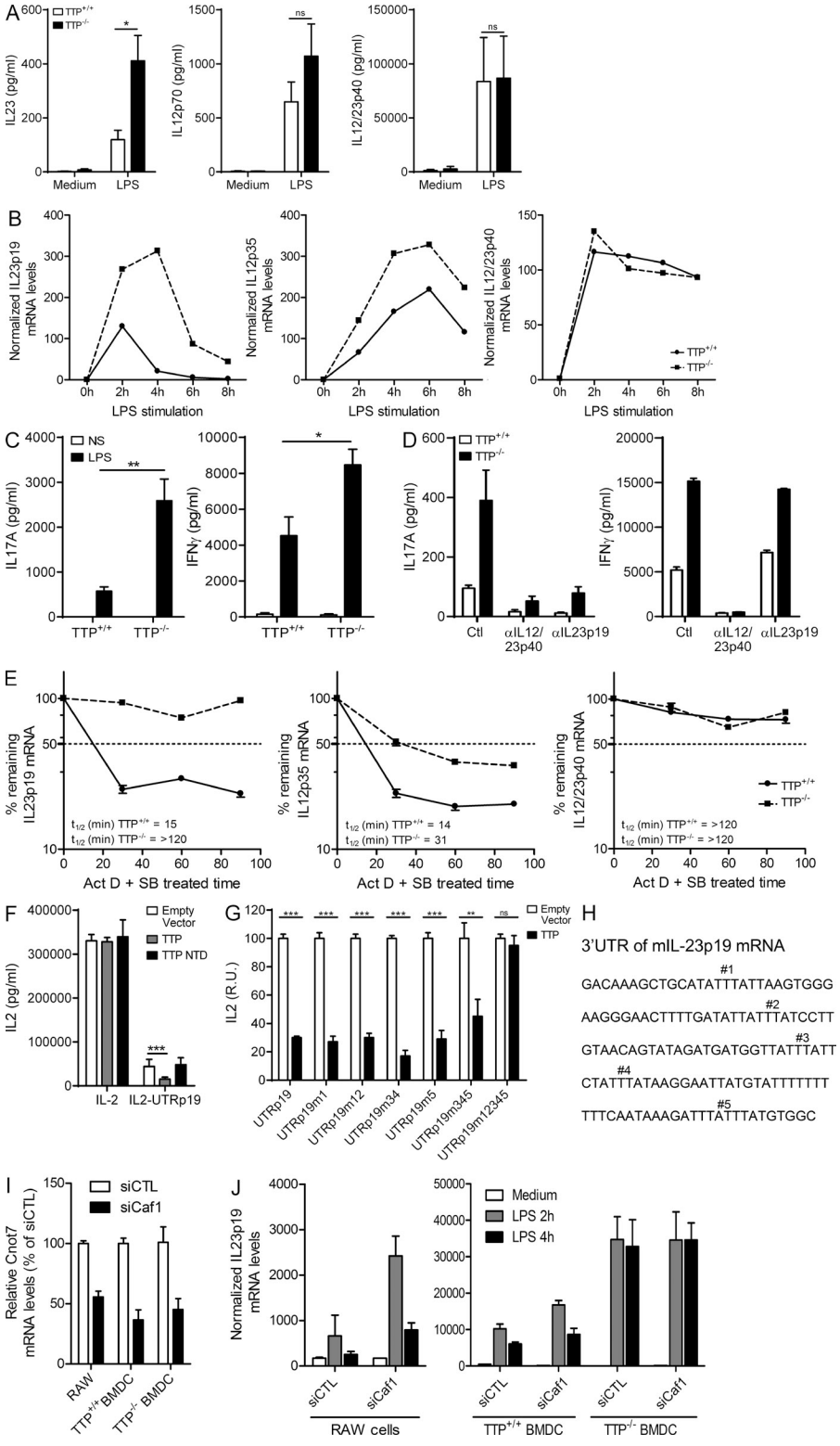

Figure 1. TTP regulates the production of IL23 in BMDCs. BMDCs from TTP$^{+/+}$ or TTP$^{-/-}$ mice were incubated in medium alone or stimulated with 100 ng/ml LPS. (A) Supernatants were collected after 16 h and analyzed for IL23, IL12p70, and IL12/23p40 levels by ELISA. Mean ± SEM of six independent experiments is shown. (B) Total RNA was extracted and analyzed by real-time RT-PCR. One experiment representative of six is shown. (C and D) Spleen cells from TLR4$^{-/-}$ mice were cultured in presence of supernatant from nonstimulated or LPS-stimulated DCs. When indicated, neutralizing antibodies for IL12/23p40, IL23p19, or control IgG (2 µg/ml) were added. After 3 d, supernatants were collected and analyzed for IL17A and IFN-γ levels by ELISA. Mean ± SEM of two experiments performed in triplicate (C) or triplicates from one representative experiment of three (D) is shown. (E) DCs from TTP$^{+/+}$ or TTP$^{-/-}$ mice were stimulated with 100 ng/ml LPS. After 2 h of stimulation, 10 µg/ml actinomycin D and 1 µM SB202190 were added for the indicated time. Total RNA was extracted and analyzed by real-time RT-PCR. The results represent mean ± SEM of triplicates from one representative experiment of five. (F and G) HEK-293 cells were cotransfected with 400 ng of the indicated reporter plasmid and 100 ng of the indicated expression vector. 24 h after transfection, culture medium was replaced by fresh medium, and 16 h later supernatant were collected and analyzed for IL2 levels by ELISA. Mean ± SEM from three experiments performed in triplicate is shown. (H) Representation of the 3′UTR of the murine IL23p19 mRNA. (I and J) Knockdown experiments were performed by nucleofection of 1 µM Caf1 or control (CTL) siRNA. 24 h later, cells were stimulated as indicated. Total RNA was extracted and analyzed by real-time RT-PCR. The results represent mean ± SEM of triplicates from one representative experiment of two. *, $P < 0.05$; **, $P < 0.01$; ***, $P < 0.001$; ns, not significant.

(Fig. 1 F). Overexpression of TTP, but not of a truncated, inactive form of TTP (TTP NTD), led to a further decrease of IL2 production driven by the 3′UTRp19-containing plasmid (Fig. 1 F). Site-directed mutagenesis revealed that all five AREs had to be mutated to completely abrogate the destabilizing effect of TTP (Fig. 1 G). These results are consistent with recent observations from Qian et al. (2011) indicating that multiple AREs mediate IL23 mRNA instability in response to IFN-γ. TTP-mediated mRNA decay requires the recruitment of a poly(A) nuclease complex containing CAF1

(CCR4-associated factor 1; Zheng et al., 2008). We depleted CAF1 protein in RAW cells by knocking down the *Cnot7* gene and observed increased LPS-induced IL23p19 mRNA expression in this condition (Fig. 1, I and J). We repeated these experiments in WT BMDCs and confirmed this trend. Importantly, IL23p19 mRNA expression was not enhanced upon CAF1 depletion in $TTP^{-/-}$ BMDCs. Collectively, our experiments confirm the direct role of TTP on IL23p19 mRNA decay through CAF1-dependent deadenylation and indicate that such a mechanism is critical to control IL23 production in LPS-stimulated BMDCs.

Dysregulated IL23 production in vivo is associated with enhanced IL17 and IL22 responses

TTP deficiency leads to the spontaneous development of a complex inflammatory syndrome that combines cachexia, dermatitis, arthritis, conjunctivitis, and myeloid hyperplasia (Taylor et al., 1996). Dermatitis is characterized by orthokeratotic hyperkeratosis, acanthosis, and neutrophil infiltrates, features which are compatible with local IL23 production (Chan et al., 2006). Moreover, ubiquitous expression of IL23p19 in transgenic mice results in weight loss, infertility, and inflammation in multiple organs, including skin (Wiekowski et al., 2001). Based on these observations, we analyzed IL23p19 mRNA and protein expression within skin lesions of $TTP^{-/-}$ mice. We observed increased expression of IL23p19 mRNA in comparison with healthy skin from WT mice (Fig. 2 A). By immunohistochemistry, we were able to detect IL23p19-positive cells in the inflamed epidermis of $TTP^{-/-}$ mice, which were absent in the skin of $TTP^{+/+}$ mice (Fig. 2 B). In contrast, IL12/23p40 mRNA expression in the skin of $TTP^{-/-}$ mice was comparable to WT mice (Fig. 2 A). Accordingly, we also detected high IL17A and IL22 mRNA levels within skin lesions and draining LNs (dLNs; Fig. 2 C) of mutant mice. Of note, these two cytokines are directly implicated in IL23-induced skin inflammation (Zheng et al., 2007; Rizzo et al., 2011). In contrast, IFN-γ mRNA levels were comparable to that observed in healthy skin and dLNs, whereas increased TNF mRNA expression was confined to inflamed skin (Fig. 2 C). TNF has been considered as the major effector cytokine responsible for the inflammatory syndrome observed in TTP-deficient mice. Although in vitro data largely confirm the negative influence of TTP on TNF expression, our observations concur with previous studies indicating that in vivo, absence of negative regulation by TTP leads to a selective elevated expression of TNF in inflamed tissues (skin, in the present study, or liver, as shown in Kaplan et al., 2011). Notably, expression of TNF in lymphoid tissues (dLN, this study, and spleen and BM in Kaplan et al., 2011) was not affected by lack of TTP expression (Kaplan et al., 2011). Herein, we demonstrate a significant up-regulation of TNF mRNA expression at the inflammation site.

We next analyzed ex vivo cytokine production of CD4 T cells from the spleen and dLNs of $TTP^{+/+}$ and $TTP^{-/-}$ mice. We observed that the frequencies of $IL17A^+$ and $IL22^+$ CD4 T cells were increased in dLNs but not the spleen of $TTP^{-/-}$ mice when compared with their WT counterpart. (Fig. 2 D). The slight increase in the frequency of IFN-γ–producing CD4 T cells did not reach statistical significance, whereas numbers of TNF^+ CD4 T cells were comparable in both groups (Fig. 2 D). As TTP could directly influence cytokine production in a T cell–intrinsic fashion, we sorted naive CD4 T cells from WT or $TTP^{-/-}$ mice and cultured them in neutral (Th0) or polarizing conditions as indicated. After 3 d of culture in Th17- or Th22-promoting media, activated T cells produced similar amounts of IL17A and IL22 in both groups at the protein or mRNA levels (Fig. 2 E and not depicted). Consistent with previous results (Ogilvie et al., 2009), absence of TTP in CD4 T cells led to increased IFN-γ production in Th1 cells (Fig. 2 E). These results indicate that $TTP^{-/-}$ CD4 T cells are not intrinsically biased toward Th17 or Th22 differentiation.

IL17A-producing γδ T cells are important effectors of inflammation in psoriatic skin (Cai et al., 2011). We found increased frequencies of $IL17A^+$ and $IL22^+$ γδ T cells in dLNs and skin lesions of $TTP^{-/-}$ mice (Fig. 2 F). Furthermore, infiltrating γδ T cells also produced higher levels of IFN-γ and TNF, confirming the highly inflammatory nature of these cells (Fig. 2 F). Interestingly, we observed that a significant proportion of $CD3^-CD4^+$ cells produced IL17A and IL22 in the spleen and dLNs of $TTP^{-/-}$ mice (Fig. 2 G). These cells might correspond to IL23-responsive innate lymphoid populations (Spits and Di Santo, 2011). Altogether, these observations indicate that inflammation that develops in absence of TTP is characterized by local IL17A and IL22 overproduction, a finding consistent with a potential pathogenic role of IL23 in this syndrome.

IL23 plays a critical role in the pathogenesis of the TTP deficiency syndrome

To elucidate the role of dysregulated IL23 production in the development of TTP deficiency syndrome, we crossed $TTP^{-/-}$ mice with $IL23p19^{-/-}$ mice. A cardinal feature of $TTP^{-/-}$ mice is their low body weight and fat content, as illustrated by their lack of weight gain after 3 wk of age (Fig. 3 A). Remarkably, $IL23p19^{-/-}TTP^{-/-}$ mice maintained growth curves identical to $TTP^{+/+}$ (Fig. 3 A). Furthermore, none of the $IL23p19^{-/-}TTP^{-/-}$ mice displayed signs of dermatitis or arthritis, whereas all $TTP^{-/-}$ mice developed at least one of these clinical manifestations during the observation period (6 mo). Histological analysis of the skin indicated that hyperkeratosis and cell infiltration observed in $TTP^{-/-}$ mice were completely absent in the skin of $IL23p19^{-/-}TTP^{-/-}$ mice (Fig. 3 B). Similarly, histological analyses revealed a lack of typical joint inflammation in $IL23p19^{-/-}TTP^{-/-}$ mice when compared with $TTP^{-/-}$ mice (Fig. 3 C). We obtained similar results when $TTP^{-/-}$ mice were treated with neutralizing IL-12/23p40 antibody from 2 wk of age (250 µg, twice a week; not depicted), strongly supporting the notion that the absence of pathology in $IL23p19^{-/-}TTP^{-/-}$ mice was secondary to the loss of IL23 expression and not a consequence of genetic background differences. To confirm the

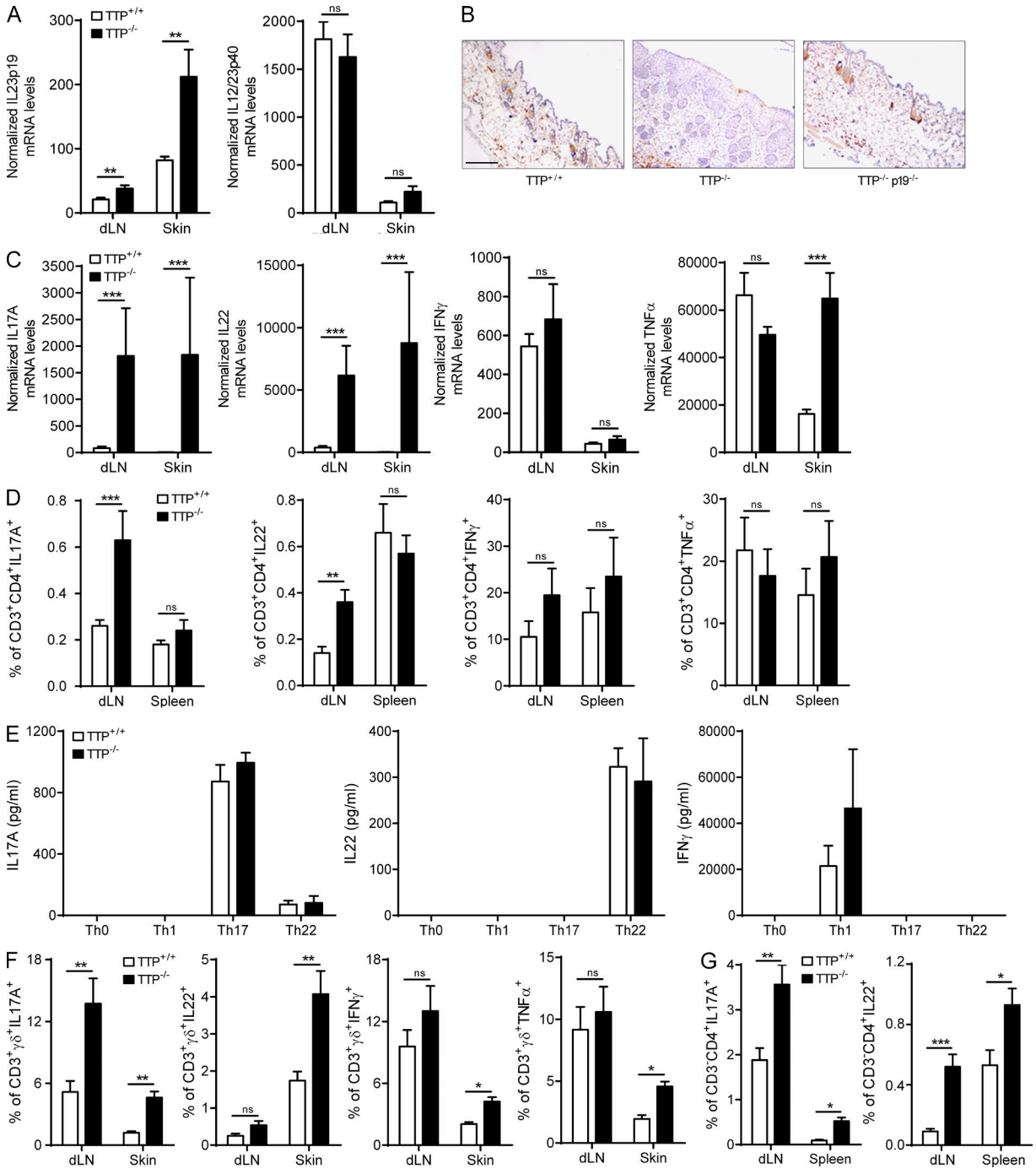

Figure 2. Enhanced IL17 and IL22 responses as consequence of the increased IL23 production. (A) Total RNA from dLN or skin of $TTP^{+/+}$ or $TTP^{-/-}$ mice was extracted and analyzed by real-time RT-PCR. Mean ± SEM from 10–15 mice is shown. (B) Representative IL23p19-stained sections of the skin of $TTP^{+/+}$, $TTP^{-/-}$, or $p19^{-/-}$ mice. Bar, 100 µm. (C) Total RNA from dLN or skin of $TTP^{+/+}$ or $TTP^{-/-}$ mice was extracted and analyzed by real-time RT-PCR. Mean ± SEM from 4–10 mice is shown. (D and G) Intracellular IL17A, IL22, IFN-γ, or TNF production assessed by flow cytometry on dLN and spleen cell suspensions of $TTP^{+/+}$ and $TTP^{-/-}$ mice stimulated by PMA/ionomycin for 4 h. Mean ± SEM from 6–10 mice is shown. (E) Naive CD4 T cells were stimulated with anti-CD3 and anti-CD28 and culture for 3 d under Th0, Th1, Th17, or Th22 conditions. Supernatants were collected analyzed for IL17A, IL22, and IFN-γ levels by ELISA. The results represent mean ± SEM of triplicates from one representative experiment of three. (F) Intracellular IL17A, IL22, IFN-γ, or TNF production assessed by flow cytometry on dLN and skin cell suspensions of $TTP^{+/+}$ and $TTP^{-/-}$ mice stimulated by PMA/ionomycin for 4 h. Mean ± SEM from 6–10 mice is shown. *, $P < 0.05$; **, $P < 0.01$; ***, $P < 0.001$; ns, not significant.

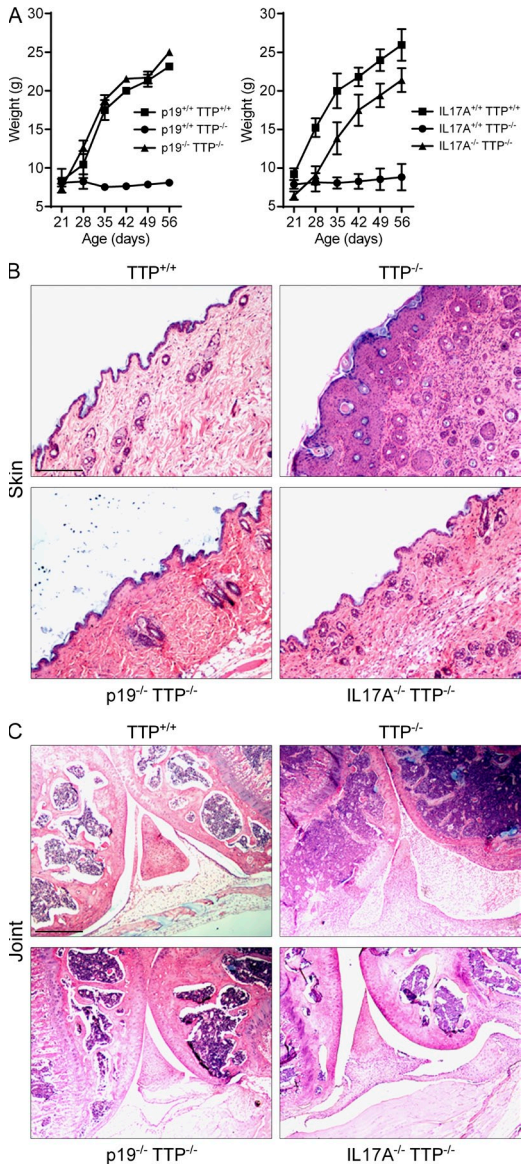

Figure 3. TTP deficiency syndrome development abolished in absence of IL23. (A) Growth curves of IL23p19$^{+/+}$ TTP$^{+/+}$, IL23p19$^{+/+}$ TTP$^{-/-}$, and IL23p19$^{-/-}$ TTP$^{-/-}$ male mice (left), and growth curves of IL17A$^{+/+}$ TTP$^{+/+}$, IL17A$^{+/+}$ TTP$^{-/-}$, and IL17A$^{-/-}$ TTP$^{-/-}$ male mice (right). Similar data were obtained with female mice (not depicted). For these experiments, p19$^{+/-}$ TTP$^{+/-}$ mice or IL17A$^{+/-}$ TTP$^{+/-}$ mice were used as breeders and we compared IL23p19$^{+/+}$ TTP$^{-/-}$ with IL23p19$^{-/-}$ TTP$^{-/-}$ littermates or IL17A$^{+/+}$ TTP$^{-/-}$ with IL17A$^{-/-}$ TTP$^{-/-}$ littermates. Mean ± SEM from ≥9 mice is shown. (B and C) Representative H&E-stained sections of the skin or the joint of TTP$^{+/+}$, TTP$^{-/-}$, IL23p19$^{-/-}$ TTP$^{-/-}$, and IL17A$^{-/-}$ TTP$^{-/-}$ mice. Bars, 100 µm.

important role of IL23 in this model, we generated double KO mice lacking expression of both TTP and IL17A. IL17A$^{-/-}$ TTP$^{-/-}$ mice did no display significant weight loss nor signs of arthritis and dermatitis (Fig. 3, A–C), confirming the functional role of the IL23–IL17 axis in this inflammatory model.

The phenotype of IL23$^{-/-}$TTP$^{-/-}$ mice was highly unexpected given the critical and direct role of TTP on TNF mRNA decay. Indeed, TNF neutralization or genetic ablation completely prevents the development of this pathology (Taylor et al., 1996; Carballo and Blackshear, 2001). There is an intimate cross talk between TNF and IL23 in the context of autoimmunity. Treatment of psoriasis or arthritis by TNF neutralization leads to decreased IL23p19 expression at the lesion site (Zaba et al., 2007; Lina et al., 2011), whereas mouse models indicate that IL23-driven epidermal hyperplasia is mediated by TNF (Chan et al., 2006). Given that both cytokines represent direct targets of TTP, this model of spontaneous inflammation represents an ideal setting to further study the interplay between these two cytokines. To this end, we analyzed mice lacking expression of TTP and TNF receptor 1 and 2 expression (TNFR1/2$^{-/-}$TTP$^{-/-}$ mice). Absence of TNF signaling resulted in a significant decrease in IL23p19, but not IL12/23p40, expression in skin lesions and dLNs, revealing a positive and specific feedback loop between TNF and IL23p19 in TTP$^{-/-}$ mice (Fig. 4 A).

Expression of IL17A and IL22 mRNA (Fig. 4 B), and frequencies of IL17A- and IL22-producing CD4 T or γδ T cells (Fig. 4, C and D) within peripheral LN or skin were found to be completely dependent on both IL23p19 and TNF signaling. Similarly, TNF mRNA levels within skin lesions were reduced in the absence of IL23, IL17A, and TNFR expression (Fig. 4 B). No impact was observed on numbers of TNF-producing cells at this site of inflammation (unpublished data), suggesting that other cell types, such as myeloid cells, constitute the source of this cytokine. Regarding IFN-γ production, both mRNA levels and CD4^{+} T cells proportions were comparable between groups (Fig. 4 B and not depicted).

Absence of TTP also leads to myeloid hyperplasia, characterized by increased proportions of F4/80^{+} macrophages and GR1^{+} neutrophils in the BM and the spleen (Taylor et al., 1996), accompanied by a slight reduction in B cell numbers in these lymphoid organs. This spontaneous granulocyte hyperplasia was recently shown to be secondary to the general inflammatory environment and associated with elevated circulating G-CSF levels (Kaplan et al., 2011). As previously shown, myeloid hyperplasia was absent in mice lacking both TTP and TNFR1/2 (Fig. 4, E and F). In keeping with our previous observations, lack of IL23p19 or IL17A expression also completely reverted to the hematological dysfunctions caused by TTP deficiency (Fig. 4 E). We observed that the increase in G-CSF levels in the plasma of TTP$^{-/-}$ mice was also dependent on IL23/IL17 (Fig. 4 F).

Initial studies of TTP$^{-/-}$ mice focused on local inflammation of joints, but Adamopoulos et al. (2011) demonstrate that systemic exposure to IL23 by hydrodynamic delivery in adult mice causes severe arthritis accompanied by a general bone loss. We therefore evaluated the overall mineralization of the skeleton by positron emission tomography (PET)–CT scan using [^{18}F]-NaF. We observed that TTP$^{-/-}$ develop strong osteopenia, associated with increased uptake of the tracer, suggestive of active bone remodeling. Bone density was globally

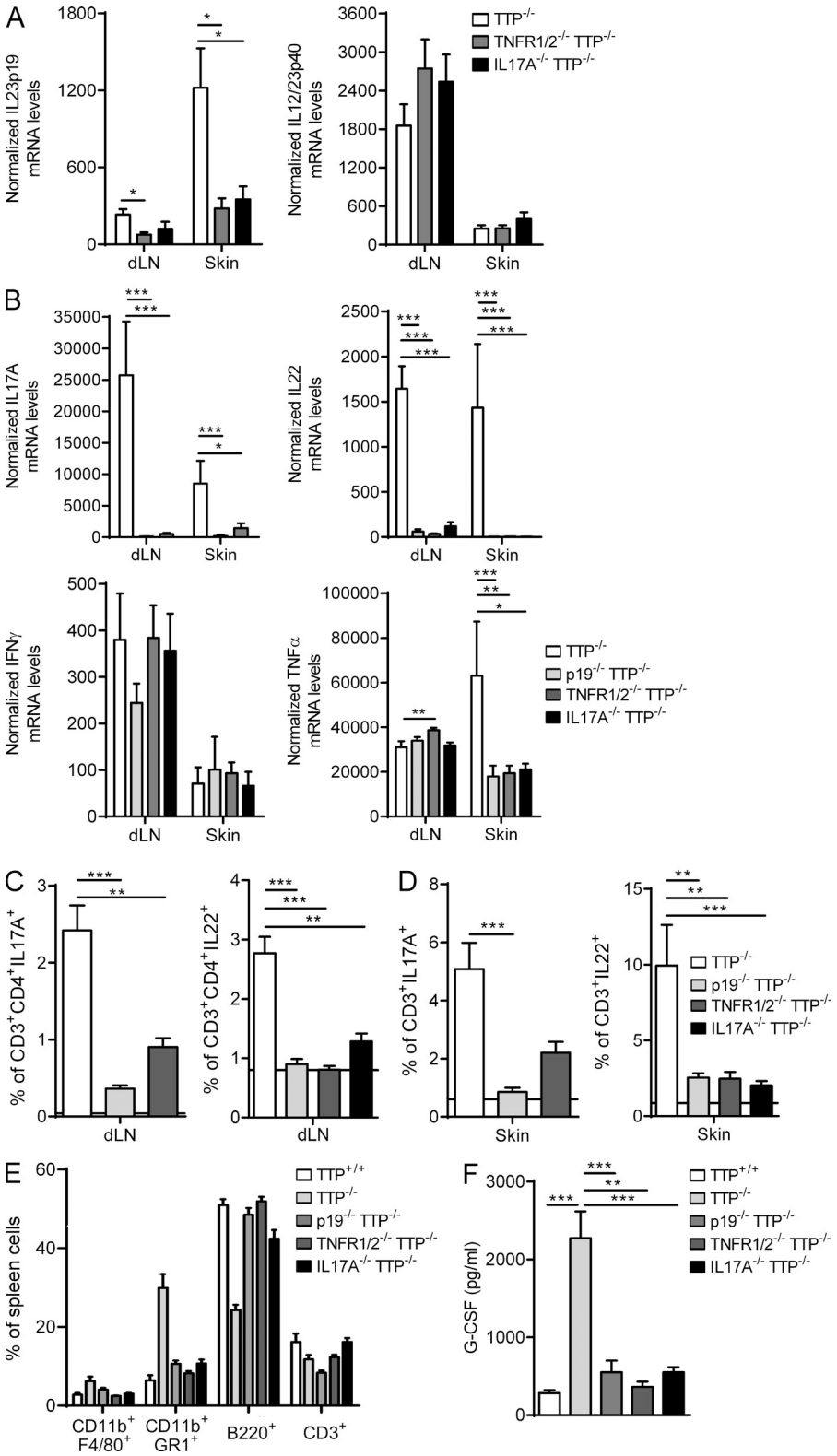

Figure 4. Production of IL17A and IL22 in TTP$^{-/-}$ mice is IL23 dependent. (A and B) Total RNA from dLN or skin of TTP$^{-/-}$, IL23p19$^{-/-}$ TTP$^{-/-}$, TNFR1/2$^{-/-}$ TTP$^{-/-}$, and IL17A$^{-/-}$ TTP$^{-/-}$ mice was extracted and analyzed by real-time RT-PCR. Mean ± SEM from 6–10 mice is shown. (C and D) Intracellular IL-17A or IL22 production assessed by flow cytometry on dLN and skin cell suspensions of TTP$^{-/-}$, IL23p19$^{-/-}$ TTP$^{-/-}$, TNFR1/2$^{-/-}$ TTP$^{-/-}$, and IL17A$^{-/-}$ TTP$^{-/-}$ mice stimulated by PMA/ionomycin for 4 h. Mean ± SEM from 6–14 mice is shown. The horizontal bar represents the background staining obtained with isotype control antibodies (E) Flow cytometric analysis of cells in the spleen of TTP$^{+/+}$, TTP$^{-/-}$, IL23p19$^{-/-}$ TTP$^{-/-}$, TNFR1/2$^{-/-}$ TTP$^{-/-}$, and IL17A$^{-/-}$ TTP$^{-/-}$ mice. Mean ± SEM from 4–8 mice is shown. (F) ELISA analysis of the G-CSF present in sera of TTP$^{+/+}$, TTP$^{-/-}$, IL23p19$^{-/-}$ TTP$^{-/-}$, TNFR1/2$^{-/-}$ TTP$^{-/-}$, and IL17A$^{-/-}$ TTP$^{-/-}$ mice. Mean ± SEM from 12–20 mice is shown. Significant statistics are shown: *, $P < 0.05$; **, $P < 0.01$; ***, $P < 0.001$.

normalized in absence of IL23. In comparison with TTP$^{-/-}$ mice, [^{18}F]-NaF uptake was decreased in TTP$^{-/-}$IL23p19$^{-/-}$ animals, suggesting that IL23 also contributes to bone remodeling in this model (Videos 1–6).

In conclusion, most of the aspects of the TTP deficiency syndrome were found to be IL23 dependent. In addition to this striking observation, we also identified IL17A as a key IL23-induced cytokine implicated in the amplification of the

inflammatory processes. Our experiments suggest that TTP directly regulates the production of both TNF and IL23, which act together in a nonredundant fashion to promote IL17A-driven inflammation. Interestingly, we found that IL23p19 and TNF expression in the skin (Fig. 4, A and B) were greatly reduced in absence of IL17A. This observation is consistent with the capacity of IL17A to enhance TNF-induced expression of IL23p19 by human synoviocytes and dermal fibroblasts derived from rheumatoid arthritis patients (Goldberg et al., 2009). In consequence, IL22 mRNA levels (Fig. 4 B) and frequencies of IL22-producing CD4 T or γδ T cells (Fig. 4, C and D) within peripheral LN or skin were decreased in absence of this cytokine. Altogether, these results indicate that IL17A acts as key effector cytokine in the TTP deficiency syndrome. This model reemphasizes TTP and regulators of TTP as potential therapeutic targets in the context of arthritis and psoriasis, as it will affect expression of both inflammatory cytokines.

Interestingly, recent evidence indicates that selective ablation of TTP in macrophage/granulocyte lineages is not sufficient to drive autoimmune inflammation (Kratochvill et al., 2011; Qiu et al., 2012). Previous studies showed that transfer of $TTP^{-/-}$ BM in $RAG^{-/-}$ mice could recapitulate the full syndrome, indicating the role of TTP in hematopoietic cells (Carballo et al., 1997). TTP is expressed in T lymphocytes and could mediate mRNA decay of several T cell–derived cytokines, such as IL2, IFN-γ, or IL17 (Ogilvie et al., 2005, 2009; Lee et al., 2012). We confirmed that upon Th1 differentiation, $TTP^{-/-}$ naive CD4 T cells tend to produce higher levels of IFN-γ. However, neither IL17A nor IL22 production was increased upon polarizing conditions. These results indicate that exacerbated Th17 and Th22 responses in the absence of TTP are not an intrinsic property of CD4 T cells. Other cell populations might therefore be implicated in the development of this autoimmune pathology. Infiltrating DCs are critical to maintain Th17 responses in the context of EAE (Huang et al., 2012). Inflammatory dermal DCs expressing TNF and IL23 are found in psoriatic skin samples (Hänsel et al., 2011). Preliminary experiments indicate that in inflamed $TTP^{-/-}$ skin, both F4/80- and CD11c-positive cells stain for IL23. Hence, the role of TTP-mediated TNF and IL23 regulation should be addressed in specific DC subpopulations.

The IL23–IL17 axis is also implicated in the regulation of granulopoiesis through induction of G-CSF (Stark et al., 2005). We provide evidence that myeloid hyperplasia is also a feature of the TTP deficiency syndrome that can be the consequence of dysregulated IL23 production.

Both IL12p35 and IL12/23p40 are highly regulated at the transcriptional and epigenetic levels (Goriely et al., 2008). TTP-mediated mRNA destabilization is not implicated in IL12/23p40 regulation and plays a minor role for IL12p35. In sharp contrast, IL23p19 is a primary response gene that strongly relies on posttranscriptional regulation. Given the central role of IL23 in inflammatory bowel diseases, multiple sclerosis, psoriasis, or arthritis, our observations have important implications for the development of antiinflammatory therapies targeting this cytokine.

MATERIALS AND METHODS

Mice. TTP (*Zfp36*)-deficient and TNFR1/2$^{-/-}$ $TTP^{-/-}$ mice on mixed 129/Sv-C57BL/6 background were obtained from P.J. Blackshear. IL23p19- and IL17A-deficient mice on C57BL/6 background were obtained from Genentech and Y. Iwakura (Institute for Medical Science, Tokyo, Japan), respectively. 129/Sv-C57BL/6 $TTP^{-/-}$ mice were maintained as a 129/Sv-C57BL/6 $TTP^{+/-}$ colony, as homozygous mice are not fertile. Experiments on $TTP^{-/-}$ or IL23p19-deficient or IL17A-deficient backgrounds were performed using littermates as controls. Mice were bred and maintained according to institutional guidelines.

Cells and reagents. Murine BMDCs were generated as previously described (Goriely et al., 2006). The HEK-293 human kidney cell line was obtained from LGC Promochem. Ultra-Pure LPS from *E. coli* (0111:B4) was obtained from InvivoGen. Actinomycin D and SB202190 were obtained from Sigma-Aldrich and EMD Millipore, respectively.

Plasmid constructs. A 656-bp fragment of the *IL-23*(*p19*) gene (nt 1290/1945) was amplified by PCR from mouse genomic DNA and subsequently cloned as an *EcoRI* insert into the pCDNA3.1 vector containing the coding sequence of the murine IL2 to generate the UTRp19 reporter plasmid. The plasmids UTRp19m1, UTRp19m12, UTRp19m34, UTRp19m5, UTRp19m345, and UTRp19m12345 are derivatives of UTRp19 in which the ARE site was altered by the QuikChange Lightning Site-Directed Mutagenesis kit (Agilent Technologies). For each ARE element, the two T nucleotides flanking the ATTTA sequence were changed in nucleotide G. pCDNA3.1-mIL2 expression vector contains the murine IL2 coding sequence, pCDNA3.1-TTP expression vector contains the TTP coding sequence, and pCDNA3.1-TTP NTD expression vector contains the first 102 amino acids of the TTP coding sequence.

Quantification of cytokine production in sera and culture supernatants. Murine cytokines (IL23, IL12/23p40, IL12p70, IL2, IL17, IL22, and IFN-γ) levels were determined in cell-free supernatants using Duoset ELISA (R&D Systems) with detection limits of 30 pg/ml. G-CSF plasma levels were quantified using Quantikine ELISA kit (R&D Systems) with detection limits of 15 pg/ml.

RNA purification and real-time RT-PCR. Total RNA from cells and tissues was extracted using a MagNA Pure LC RNA High Performance Isolation kit and MagNA Pure LC RNA Isolation kit III, respectively (Roche). RT and real-time PCR reactions were then performed using Taqman RNA amplification kit (one-step procedure) on a LightCycler 480 Real-Time PCR system (Roche). mRNA levels were expressed as absolute number of copies normalized against β-actin mRNA. This was achieved by generating standard curves from serial dilutions of PCR-generated standards. The sequences of primers and probes were: β-actin: 5′-TCCTGAGCGCAAGTACTCTGT-3′, 5′-CTGATCCACATCTGCTGGAAG-3′, and probe 5′-ATCGGTGGCTCCATCCTGGC-3′; IFN-γ: 5′-GGATGCATTCATGAGTATTGC-3′, 5′-GCTTCCTGAGGCTGGATTC-3′, and probe 5′-TTTGAGGTCAACAACCCACAGGTCCA-3′; IL12/23p40: 5′-GTTCAACATCAAGAGCAGTAGCA-3′, 5′-CTGCAGACAGAGACGCCATT-3′, and probe 5′-CCCTGACTCTCGGGCAGTGACA-3′; IL12p35: 5′-CTTAGCCAGTCCCGAAACCT-3′, 5′-TTGGTCCCGTGTGATGTCT-3′, and probe 5′-TCTGGCCGTCTTCACCATGTCA-3′; IL17a: 5′-GCTCCAGAAGGCCCTCAG-3′, 5′-CTTTCCCTCCGCATTGACA-3′, and probe 5′-ACCTCAACCGTTCCACGTCACCCTG-3′; IL22: 5′-ACAGGTTCCAGCCCTACATG-3′, 5′-GTCGTCACCGCTGATGTG-3′, and probe 5′-TGGTACCTTTCCTGACCAAACTCAGCA-3′; IL23p19: 5′-CCCGTATCCAGTGTGAAGATG-3′, 5′-CCCTTTGAAGATGTCAGAGTCA-3′, and probe 5′-CCACAAGGACTCAAGGACAACAGCC-3′; TNF: 5′-CAGACCCTCACACTCAGATCA-3′, 5′-CACTTGGTGGTTTGCTACGA-3′, and probe 5′-TCGAGTGACAAGCCTGTAGCCCA-3′. The primers and probe mix for the quantification of Cnot7 mRNA (Mm00516123_m1) were purchased from Life Technologies.

Transient transfection and luciferase assays. HEK-293 cells were transfected using FuGENE-6 (Roche) as previously described (Goriely et al., 2006). Promoter activities were analyzed with the quantification of mouse IL2 production in the cell-free supernatant using Duoset ELISA (R&D Systems).

siRNA nucleofection. For siRNA transfection, Cell Line Nucleofector kits T (T-001 program) and V (Y-001 program) were used for RAW cells and BMDCs, respectively, using a Nucleofector 2b apparatus (Lonza). Mouse *Cnot7* (encoding CAF1) ON-TARGET plus siRNA (L-059073-00-0005) and nontargeting siRNA (D-001810-10-05) SMART pools were purchased from Thermo Fisher Scientific.

Spleen cell cultures. Single cell suspensions of spleen were prepared from TLR4$^{-/-}$ mice. 2 × 10^6 cells/ml were cultured with 100 U/ml IL2 (Proleukin) in the presence or absence of supernatant of BMDCs culture for 72 h, after which supernatant were collected and analyzed for cytokines production using ELISA. Anti-IL23p19 (Polyclonal goat IgG, AF1619) and anti-IL12/23p40 (C17.8) antibodies were purchased from R&D Systems and BD, respectively.

T cell purification. Naive CD4$^+$ T cells were purified by pre-enrichment of CD4$^+$ T cells from spleens by magnetic-activated cell sorting (Dynal CD4$^+$ T cell negative isolation kit; Invitrogen) and sorting by flow cytometry for CD4$^+$CD62L$^+$CD25$^-$ T cells (FACSAria; BD) after staining with anti-CD4 (RM4-5), anti-CD62L (MEL-14), and anti-CD25 (PC61; all from BD).

T cell cultures. All cultures were incubated in IMDM with 10% (vol/vol) FCS, 2 mM L-glutamine, 1 mM sodium pyruvate, 0.1 mM nonessential amino acids, 40 μM β-mercaptoethanol, 100 U/ml penicillin, and 100 U/ml streptomycin (all from Lonza). Culture plates were coated for 2 h with 5 μg/ml anti-CD3 in PBS (145-2C11; BD). Cells were plated at a density of 10^6 cells per ml and were stimulated with 1 μg/ml anti-CD28 (37.51, BD Biosciences). T cells were cultured for 3 d in Th0 conditions (10 μg/ml anti–IFN-γ [R4-6A2; BD], and 10 μg/ml anti-IL4 [11B11; BD]), Th1 conditions (10 ng/ml recombinant IL12 [R&D Systems] plus 10 μg/ml anti-IL4), Th17 conditions (2.5 ng/ml of recombinant human TGF-β [R&D Systems] and 10 ng/ml of recombinant IL6 [R&D Systems] plus anti–IFN-γ and anti-IL4), or Th22 (20 ng/ml of recombinant IL6 and 10 ng/ml of recombinant IL23 [R&D Systems] plus anti–IFN-γ and anti-IL4).

Skin cell isolation. Skin was incubated in 2.5 mg/ml collagenase I (Sigma-Aldrich). Tissues were dissociated with the gentle MACS Dissociator (Miltenyi Biotec) to obtain single-cell suspensions.

Restimulation and intracellular staining. Spleen cells, dLNs, or skin cells were stimulated for 4 h with 25 ng/ml PMA (Sigma-Aldrich) and 500 ng/ml ionomycin (Sigma-Aldrich) with the addition of 5 μg/ml Brefeldin A (Sigma-Aldrich) for the last 2 h. Cells were first stained for surface antigens (CD4 PB [RM4-5], CD3 Percp [SP34-2], and γ/δ TCR FITC [GL3], all from BD) and then treated with Cytofix/Cytoperm (BD) according to the manufacturer's directions. Intracellular cytokine staining was performed using anti-IL17A AF647 (TC11-18H10; BD), anti-IL22 PE (clone 1H8PW5R; eBioscience), TNF APC (MP6-XT22; BD), or anti–IFN-γ PE (XMG1.2; BD).

Hematopoietic system analysis. Spleen cells were stained using anti-CD11b PE (M1/70), anti-GR1 APC (RB6-8C5), anti-CD3 Percp (SP34-2), and anti-B220 FITC (RA3-6B2). All antibodies were purchased from BD. Antibody directed against F4/80 PB (CI:A3-1) was purchased from AbD Serotec.

Histological analysis. Mouse tissues were fixed in 4% buffered formalin. When required, tissues were decalcified in 30% formic acid. Fixed tissues were embedded in paraffin, sectioned, and stained with H&E. Staining was performed using goat anti–mouse IL23p19 antibody (R&D Systems) and biotin-conjugated donkey anti–goat IgG (Jackson ImmunoResearch Laboratories) as secondary antibodies.

Statistical analysis. Mann-Whitney test or Kruskal-Wallis test (Nonparametric ANOVA) with Dunn's Multiple Comparisons tests were used for statistical calculation.

Online supplemental material. Videos 1–6 show that TTP-associated osteopenia and increased bone remodeling are dependent on IL23. Online supplemental material is available at http://www.jem.org/cgi/content/full/jem.20120707/DC1.

The Institute for Medical Immunology is sponsored by the government of the Walloon Region and GlaxoSmithKline Biologicals. This study was supported by the Fonds National de la Recherche Scientifique (FRS-FNRS, Belgium), the WELBIO, and an Interuniversity Attraction Pole of the Belgian Federal Science Policy. C. Molle is a postdoctoral fellow of the FRS-FNRS. L. Ysebrant and M. Andrianne are supported by a grant from the Télévie. S. Goriely is a research associate of the FRS-FNRS.
P.J. Blackshear is supported by the Intramural Research Program of the NIEHS, NIH.
The authors have no conflicting financial interests.

Submitted: 2 April 2012
Accepted: 23 July 2013

REFERENCES

Adamopoulos, I.E., M. Tessmer, C.C. Chao, S. Adda, D. Gorman, M. Petro, C.C. Chou, R.H. Pierce, W. Yao, N.E. Lane, et al. 2011. IL-23 is critical for induction of arthritis, osteoclast formation, and maintenance of bone mass. *J. Immunol.* 187:951–959. http://dx.doi.org/10.4049/jimmunol.1003986

Anderson, P. 2008. Post-transcriptional control of cytokine production. *Nat. Immunol.* 9:353–359. http://dx.doi.org/10.1038/ni1584

Blackshear, P.J. 2002. Tristetraprolin and other CCCH tandem zinc-finger proteins in the regulation of mRNA turnover. *Biochem. Soc. Trans.* 30:945–952. http://dx.doi.org/10.1042/BST0300945

Cai, Y., X. Shen, C. Ding, C. Qi, K. Li, X. Li, V.R. Jala, H.G. Zhang, T. Wang, J. Zheng, and J. Yan. 2011. Pivotal role of dermal IL-17-producing γδ T cells in skin inflammation. *Immunity.* 35:596–610. http://dx.doi.org/10.1016/j.immuni.2011.08.001

Carballo, E., and P.J. Blackshear. 2001. Roles of tumor necrosis factor-alpha receptor subtypes in the pathogenesis of the tristetraprolin-deficiency syndrome. *Blood.* 98:2389–2395. http://dx.doi.org/10.1182/blood.V98.8.2389

Carballo, E., G.S. Gilkeson, and P.J. Blackshear. 1997. Bone marrow transplantation reproduces the tristetraprolin-deficiency syndrome in recombination activating gene-2 (-/-) mice. Evidence that monocyte/macrophage progenitors may be responsible for TNFalpha overproduction. *J. Clin. Invest.* 100:986–995. http://dx.doi.org/10.1172/JCI119649

Carballo, E., W.S. Lai, and P.J. Blackshear. 2000. Evidence that tristetraprolin is a physiological regulator of granulocyte-macrophage colony-stimulating factor messenger RNA deadenylation and stability. *Blood.* 95:1891–1899.

Carballo, E., H. Cao, W.S. Lai, E.A. Kennington, D. Campbell, and P.J. Blackshear. 2001. Decreased sensitivity of tristetraprolin-deficient cells to p38 inhibitors suggests the involvement of tristetraprolin in the p38 signaling pathway. *J. Biol. Chem.* 276:42580–42587. http://dx.doi.org/10.1074/jbc.M104953200

Chan, J.R., W. Blumenschein, E. Murphy, C. Diveu, M. Wiekowski, S. Abbondanzo, L. Lucian, R. Geissler, S. Brodie, A.B. Kimball, et al. 2006. IL-23 stimulates epidermal hyperplasia via TNF and IL-20R2–dependent mechanisms with implications for psoriasis pathogenesis. *J. Exp. Med.* 203:2577–2587. http://dx.doi.org/10.1084/jem.20060244

Gerosa, F., B. Baldani-Guerra, L.A. Lyakh, G. Batoni, S. Esin, R.T. Winkler-Pickett, M.R. Consolaro, M. De Marchi, D. Giachino, A. Robbiano, et al. 2008. Differential regulation of interleukin 12 and interleukin 23 production in human dendritic cells. *J. Exp. Med.* 205:1447–1461. http://dx.doi.org/10.1084/jem.20071450

Goldberg, M., O. Nadiv, N. Luknar-Gabor, G. Agar, Y. Beer, and Y. Katz. 2009. Synergism between tumor necrosis factor alpha and interleukin-17 to induce IL-23 p19 expression in fibroblast-like synoviocytes. *Mol. Immunol.* 46:1854–1859. http://dx.doi.org/10.1016/j.molimm.2009.01.004

Goriely, S., C. Molle, M. Nguyen, V. Albarani, N.O. Haddou, R. Lin, D. De Wit, V. Flamand, F. Willems, and M. Goldman. 2006. Interferon regulatory factor 3 is involved in Toll-like receptor 4 (TLR4)- and TLR3-induced IL-12p35 gene activation. *Blood*. 107:1078–1084. http://dx.doi.org/10.1182/blood-2005-06-2416

Goriely, S., M.F. Neurath, and M. Goldman. 2008. How microorganisms tip the balance between interleukin-12 family members. *Nat. Rev. Immunol.* 8:81–86. http://dx.doi.org/10.1038/nri2225

Hänsel, A., C. Günther, J. Ingwersen, J. Starke, M. Schmitz, M. Bachmann, M. Meurer, E.P. Rieber, and K. Schäkel. 2011. Human slan (6-sulfo LacNAc) dendritic cells are inflammatory dermal dendritic cells in psoriasis and drive strong TH17/TH1 T-cell responses. *J. Allergy Clin. Immunol.* 127: 787–794: e1–e9. http://dx.doi.org/10.1016/j.jaci.2010.12.009

Hao, S., and D. Baltimore. 2009. The stability of mRNA influences the temporal order of the induction of genes encoding inflammatory molecules. *Nat. Immunol.* 10:281–288. http://dx.doi.org/10.1038/ni.1699

Huang, G., Y. Wang, P. Vogel, T.D. Kanneganti, K. Otsu, and H. Chi. 2012. Signaling via the kinase p38α programs dendritic cells to drive TH17 differentiation and autoimmune inflammation. *Nat. Immunol.* 13:152–161. http://dx.doi.org/10.1038/ni.2207

Kang, J.G., M.J. Amar, A.T. Remaley, J. Kwon, P.J. Blackshear, P.Y. Wang, and P.M. Hwang. 2011. Zinc finger protein tristetraprolin interacts with CCL3 mRNA and regulates tissue inflammation. *J. Immunol.* 187:2696–2701. http://dx.doi.org/10.4049/jimmunol.1101149

Kaplan, I.M., S. Morisot, D. Heiser, W.C. Cheng, M.J. Kim, and C.I. Civin. 2011. Deletion of tristetraprolin caused spontaneous reactive granulopoiesis by a non-cell-autonomous mechanism without disturbing long-term hematopoietic stem cell quiescence. *J. Immunol.* 186:2826–2834. http://dx.doi.org/10.4049/jimmunol.1002806

Kastelein, R.A., C.A. Hunter, and D.J. Cua. 2007. Discovery and biology of IL-23 and IL-27: related but functionally distinct regulators of inflammation. *Annu. Rev. Immunol.* 25:221–242. http://dx.doi.org/10.1146/annurev.immunol.22.012703.104758

Kratochvill, F., C. Machacek, C. Vogl, F. Ebner, V. Sedlyarov, A.R. Gruber, H. Hartweger, R. Vielnascher, M. Karaghiosoff, T. Rülicke, et al. 2011. Tristetraprolin-driven regulatory circuit controls quality and timing of mRNA decay in inflammation. *Mol. Syst. Biol.* 7:560. http://dx.doi.org/10.1038/msb.2011.93

Lai, W.S., E. Carballo, J.R. Strum, E.A. Kennington, R.S. Phillips, and P.J. Blackshear. 1999. Evidence that tristetraprolin binds to AU-rich elements and promotes the deadenylation and destabilization of tumor necrosis factor alpha mRNA. *Mol. Cell. Biol.* 19:4311–4323.

Lee, H.H., N.A. Yoon, M.T. Vo, C.W. Kim, J.M. Woo, H.J. Cha, Y.W. Cho, B.J. Lee, W.J. Cho, and J.W. Park. 2012. Tristetraprolin down-regulates IL-17 through mRNA destabilization. *FEBS Lett.* 586:41–46. http://dx.doi.org/10.1016/j.febslet.2011.11.021

Lina, C., W. Conghua, L. Nan, and Z. Ping. 2011. Combined treatment of etanercept and MTX reverses Th1/Th2, Th17/Treg imbalance in patients with rheumatoid arthritis. *J. Clin. Immunol.* 31:596–605. http://dx.doi.org/10.1007/s10875-011-9542-6

Ogilvie, R.L., M. Abelson, H.H. Hau, I. Vlasova, P.J. Blackshear, and P.R. Bohjanen. 2005. Tristetraprolin down-regulates IL-2 gene expression through AU-rich element-mediated mRNA decay. *J. Immunol.* 174:953–961.

Ogilvie, R.L., J.R. Sternjohn, B. Rattenbacher, I.A. Vlasova, D.A. Williams, H.H. Hau, P.J. Blackshear, and P.R. Bohjanen. 2009. Tristetraprolin mediates interferon-gamma mRNA decay. *J. Biol. Chem.* 284:11216–11223. http://dx.doi.org/10.1074/jbc.M901229200

Qian, X., H. Ning, J. Zhang, D.F. Hoft, D.J. Stumpo, P.J. Blackshear, and J. Liu. 2011. Posttranscriptional regulation of IL-23 expression by IFN-gamma through tristetraprolin. *J. Immunol.* 186:6454–6464. http://dx.doi.org/10.4049/jimmunol.1002672

Qiu, L.Q., D.J. Stumpo, and P.J. Blackshear. 2012. Myeloid-specific tristetraprolin deficiency in mice results in extreme lipopolysaccharide sensitivity in an otherwise minimal phenotype. *J. Immunol.* 188:5150–5159. http://dx.doi.org/10.4049/jimmunol.1103700

Rizzo, H.L., S. Kagami, K.G. Phillips, S.E. Kurtz, S.L. Jacques, and A. Blauvelt. 2011. IL-23-mediated psoriasis-like epidermal hyperplasia is dependent on IL-17A. *J. Immunol.* 186:1495–1502. http://dx.doi.org/10.4049/jimmunol.1001001

Spits, H., and J.P. Di Santo. 2011. The expanding family of innate lymphoid cells: regulators and effectors of immunity and tissue remodeling. *Nat. Immunol.* 12:21–27. http://dx.doi.org/10.1038/ni.1962

Stark, M.A., Y. Huo, T.L. Burcin, M.A. Morris, T.S. Olson, and K. Ley. 2005. Phagocytosis of apoptotic neutrophils regulates granulopoiesis via IL-23 and IL-17. *Immunity*. 22:285–294. http://dx.doi.org/10.1016/j.immuni.2005.01.011

Taylor, G.A., E. Carballo, D.M. Lee, W.S. Lai, M.J. Thompson, D.D. Patel, D.I. Schenkman, G.S. Gilkeson, H.E. Broxmeyer, B.F. Haynes, and P.J. Blackshear. 1996. A pathogenetic role for TNF alpha in the syndrome of cachexia, arthritis, and autoimmunity resulting from tristetraprolin (TTP) deficiency. *Immunity*. 4:445–454. http://dx.doi.org/10.1016/S1074-7613(00)80411-2

Van Tubergen, E., R. Vander Broek, J. Lee, G. Wolf, T. Carey, C. Bradford, M. Prince, K.L. Kirkwood, and N.J. D'Silva. 2011. Tristetraprolin regulates interleukin-6, which is correlated with tumor progression in patients with head and neck squamous cell carcinoma. *Cancer.* 117:2677–2689. http://dx.doi.org/10.1002/cncr.25859

Wiekowski, M.T., M.W. Leach, E.W. Evans, L. Sullivan, S.C. Chen, G. Vassileva, J.F. Bazan, D.M. Gorman, R.A. Kastelein, S. Narula, and S.A. Lira. 2001. Ubiquitous transgenic expression of the IL-23 subunit p19 induces multiorgan inflammation, runting, infertility, and premature death. *J. Immunol.* 166:7563–7570.

Zaba, L.C., I. Cardinale, P. Gilleaudeau, M. Sullivan-Whalen, M. Suárez-Fariñas, J. Fuentes-Duculan, I. Novitskaya, A. Khatcherian, M.J. Bluth, M.A. Lowes, and J.G. Krueger. 2007. Amelioration of epidermal hyperplasia by TNF inhibition is associated with reduced Th17 responses. *J. Exp. Med.* 204:3183–3194. http://dx.doi.org/10.1084/jem.20071094

Zheng, D., N. Ezzeddine, C.Y. Chen, W. Zhu, X. He, and A.B. Shyu. 2008. Deadenylation is prerequisite for P-body formation and mRNA decay in mammalian cells. *J. Cell Biol.* 182:89–101. http://dx.doi.org/10.1083/jcb.200801196

Zheng, Y., D.M. Danilenko, P. Valdez, I. Kasman, J. Eastham-Anderson, J. Wu, and W. Ouyang. 2007. Interleukin-22, a T(H)17 cytokine, mediates IL-23-induced dermal inflammation and acanthosis. *Nature*. 445:648–651. http://dx.doi.org/10.1038/nature05505